Basis 1	Bravais lattice Primitive vectors 2
Primitive cell 3	Wigner-Seitz cell 4
Non-primitive unit cell 5	Honeycomb lattice 6
Oblique lattice 7	Rectangular lattice 8

The group of atoms attached to each lattice point is called the basis.

crystal structure = lattice + basis

$$\mathbf{T} = n_1\mathbf{a}_1 + n_2\mathbf{a}_2 + n_3\mathbf{a}_3$$

The vectors $\mathbf{a}_1$, $\mathbf{a}_2$ and $\mathbf{a}_3$ are called primitive vectors. The choice of $\mathbf{a}_i$ is not unique. All points of this lattice are equivalent. Has inversion symmetry.

A volume of space that, when translated through all the vectors in a Bravais lattice fills all the space without leaving voids or overlapping is called primitive cell of the lattice. Contains exactly one lattice point.

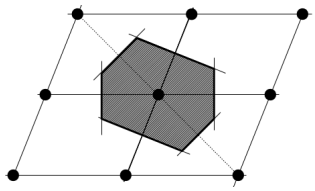

The translations form a subset of the vectors of the Bravais lattice. These unit cells may have higher symmetry than the primitive cell.

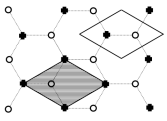

Is not a Bravais lattice as it can be viewed as a bipartite lattice formed by two hexagonal lattices and lacks inversion symmetry.

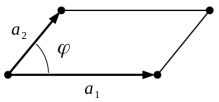

Parallelogram with no other symmetry.

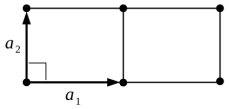

$\phi = 90°$, reflection planes and $180°$ rotations.

Square lattice

9

Hexagonal lattice

10

Centered rectangular lattice
Rhombic lattice

11

Cubic system

12

Tetragonal system

13

Orthorombic system

14

Monoclinic system

15

Triclinic system

16

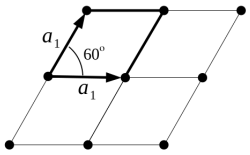

$\phi = 60°$, $a_1 = a_2$, reflection planes and 60° rotations. More isotropic than square.

10

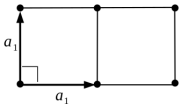

$\phi = 90°$, $a_1 = a_2$, reflection planes and 90° rotations.

9

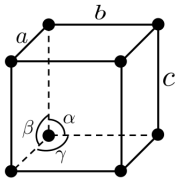

$a = b = c$ $\alpha = \beta = \gamma = 90°$

12

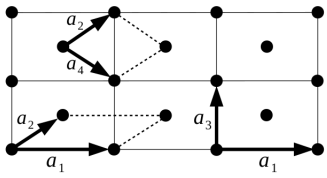

$\mathbf{a}_1$, $\mathbf{a}_2$ no reflection symmetry, $\mathbf{a}_1$, $\mathbf{a}_3$ not primitive, $\mathbf{a}_2$, $\mathbf{a}_4$ primitive.

11

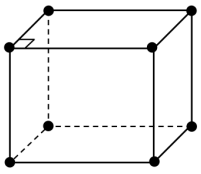

$a \neq b \neq c$
$\alpha = \beta = \gamma = 90°$

14

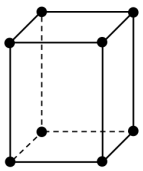

$a = b \neq c$
$\alpha = \beta = \gamma = 90°$

13

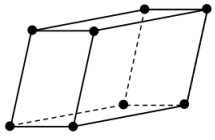

$a \neq b \neq c$
$\alpha \neq \beta \neq \gamma \neq 90°$

16

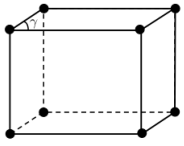

$a \neq b \neq c$
$\gamma \neq \alpha = \beta = 90°$

15

Trigonal system
Rhombohedral system

17

Hexagonal system

18

Point group
Anisotropy

19

NaCl structure

20

Hexagonal close-packed structure

21

HCP and FCC

22

Graphene structure

23

Graphite structure

24

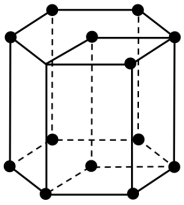

$a = b \neq c \; \alpha = \beta = 90°, \gamma = 120°$

18

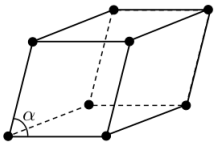

Cube stretched along its body diagonal: $a = b = c \; \alpha = \beta = \gamma \neq 90°$

17

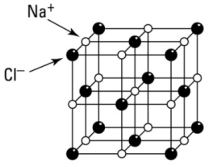

fcc, where basis consists of one Na atom and a Cl atom seperated by one-half the body diagonal.

20

The subset of the full symmetry group of the crystal that leaves a particular point fixes is called the point group.
Anisotropy in a crystal means that different directions have different properties. The anisotropy is determined by the symmetry of the directions.

19

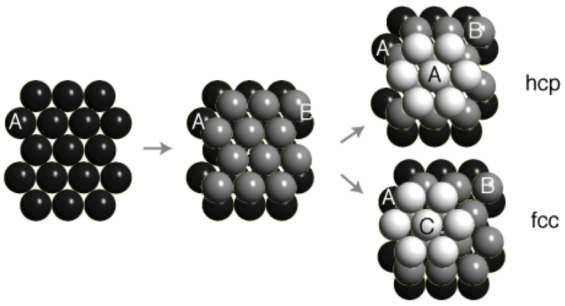

22

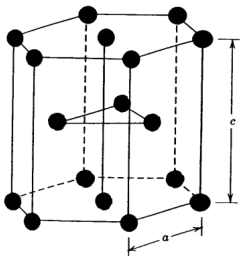

Stacking of hexagonal lattices of identical spheres, highest average density, not a Bravais lattice.

21

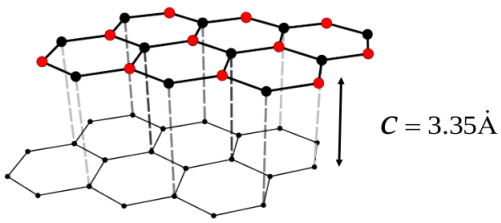

Shifted stacking of graphene layers

24

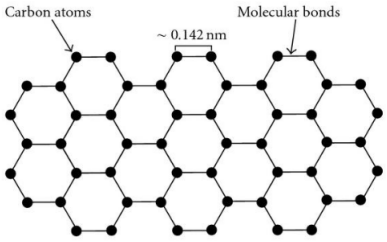

Honeycomb lattice of carbon atoms

23

Diamond structure

25

Symmetry of dielectric constant and resistivity
Elastic free energy in a tetragonal system

26

Reciprocal lattice vectors

27

Brillouin zone

28

Bloch's Theorem

29

Nearly free electron model

30

Tight binding approximation

31

Tight binding model in second quantization
and its results

32

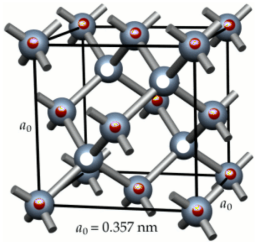

Two intercalated fcc latices diplaced along the diagonal of the cubic cell by one quarter of the unit cell diagonal. Not a Bravais lattice.

$\varepsilon_{\alpha\beta}$ and $\rho_{\alpha\beta}$ are symmetric rank 2 tensors, valid for any structure (no dependence on crystal symmetry).

$$F = \frac{\lambda}{2}(\boldsymbol{\nabla} \cdot \mathbf{u})^2 + \mu u_{\alpha\beta}^2$$

$$\mathbf{R}_n = n_1\mathbf{a}_1 + n_2\mathbf{a}_2 + n_3\mathbf{a}_3$$

$$\mathbf{G}_m \cdot \mathbf{R}_n = 2\pi N$$

The reciprocal lattice vectors are given by

$$\mathbf{G}_m = m_1\mathbf{b}_1 + m_2\mathbf{b}_2 + m_3\mathbf{b}_3$$

where

$$\mathbf{b}_i \cdot \mathbf{a}_j = 2\pi\delta_{ij}$$

The (first) Brillouin zone is defined as the Wigner-Seitz cell in the reciprocal lattice.

Electron in a periodic potential $V(r)$

$$\psi(\mathbf{r}) = \psi_{\mathbf{k}}(\mathbf{r}) = e^{i\mathbf{k}\cdot\mathbf{r}}u(\mathbf{r})$$

where $u(\mathbf{r} + \mathbf{R}_n) = u(\mathbf{r})$ is called the Bloch function.
$\Rightarrow$ For every quasi momentum $\mathbf{k}$ there are different levels $\varepsilon_l(\mathbf{k})$ in the first Brillouin zone.

Weak periodic potential $V(\mathbf{r})$

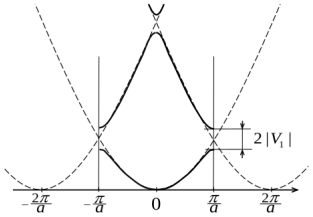

For $k \ll G_n \Rightarrow$ mass renormalization $m^* > m$.
For $k \to G/2 = \pi/a \Rightarrow$ energy gap of $2|V_1|$

Separated atoms with small orbital overlap

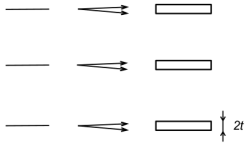

$$\varepsilon(k) = \varepsilon_0 + const - 2t\cos(ka)$$

t is exponentially small $\Rightarrow$ atomic levels expand to narrow bands and have large gaps.

$\mathcal{H} \Rightarrow$ diagonal by Fourier transformation, for small k

$$\Rightarrow \varepsilon_k = -6t - 12t' + \frac{\hbar^2}{2m^*}(k_x^2 + k_y^2 + k_z^2)$$

isotropic spectrum. Away from the bottom of the band, we get cubic symmetry. In general, the energy function in the Brillouin zone has the full point group symmetry of the crystal.

Number of orbitals in a band

33

Metals, insulators, semiconductors

34

Semiclassical dynamics

35

Bloch oscillations

36

Current densities, electrons and holes

37

Almost empty/full bands

38

Density of states

39

Specific heat in anisotropic Fermi gas

40

Valence band and conduction band

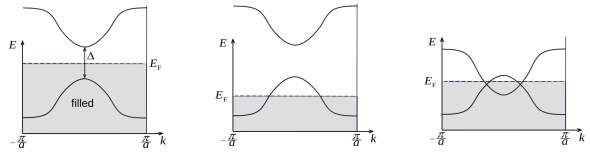

band insulator/ semiconductor | metal | semi-metal

odd number of e^- $\Rightarrow$ metal
even number of e^- and no band overlap $\Rightarrow$ insulator

34

The allowed values of the electron wave vector k are

$$k_n = \frac{2\pi}{L} n = \frac{2\pi}{a} \frac{n}{N}.$$

The total number of atomic orbitals in a band including spin is 2N.

p.25 Ziman

33

$\varepsilon_{\mathbf{k}}$ is periodic: $\varepsilon_{\mathbf{k}} = -2\tilde{t}\cos(ka)$. From

$$\hbar\dot{k} = -eE \quad \text{and} \quad \dot{x} = \frac{\partial \varepsilon_k}{\partial \hbar k}$$

$$\Rightarrow \quad x(t) = \frac{2\tilde{t}}{eE} \cos\left(\frac{eEat}{\hbar}\right)$$

The electron oscillates around its initial position. In real solids this effect is not realized due to scattering.

36

Bloch waves spatially uncertain $\Rightarrow$ wave packet description:

$$\mathbf{v}(\mathbf{k}) = \frac{\partial \varepsilon_{\mathbf{k}}}{\partial \hbar \mathbf{k}}$$

$$\hbar \frac{d\mathbf{k}}{dt} = -e\mathbf{E}(\mathbf{r},t) - \frac{e}{c}\mathbf{v}(\mathbf{k}) \times \mathbf{H}(\mathbf{r},t)$$

35

Near the bottom of the band: $\varepsilon(\mathbf{p}) = \varepsilon_0 + \mathbf{p}^2/2m^*$ and for holes $\varepsilon(\mathbf{p}) = \varepsilon_0 - \mathbf{p}^2/2m_h^*$ in a cubic crystal. Metals with small number of electrons or holes are rather rare, but found in semimetals as they have an even number of e^- and a small overlap of upper two bands. Also in nonstochiometric compounds AB_x with $x \ll 1$ where A is an insulator and the conduction electrons are coming from B.

38

The current density vanishes for filled/empty bands

$$\mathbf{j} = -2e \int_{\mathrm{BZ}} \frac{d^3k}{(2\pi)^3} n(\mathbf{k}) \frac{\partial \varepsilon_{\mathbf{k}}}{\partial \hbar \mathbf{k}}$$

as well as for the Fermi distribution. Further

$$-2e \int_{\mathrm{BZ}} \frac{d^3k}{(2\pi)^3} n(\mathbf{k})\mathbf{v}(\mathbf{k}) = 2e \int_{\mathrm{BZ}} \frac{d^3k}{(2\pi)^3} [1 - n(\mathbf{k})]\mathbf{v}(\mathbf{k})$$

thus, we can sum either over filled (electrons) states or over empty holes states.

37

$$C = \frac{1}{V} \frac{\partial}{\partial T}\bigg|_V 2V \int \varepsilon(\mathbf{p}) f(\varepsilon) \frac{d^3p}{(2\pi\hbar)^3}$$

Consider $\partial f/\partial \varepsilon$ and the particle conservation

$$C = -\int \varepsilon \frac{\partial f}{\partial \varepsilon} \left(\frac{\varepsilon - \mu}{T} + \frac{d\mu}{dT}\right) N(\varepsilon) d\varepsilon$$

which can be expanded and finally

$$\mu(T) = \mu(0) - \frac{\pi^2 T^2}{6} \frac{N'(\mu)}{N(\mu)} \qquad C = \frac{\pi^2}{3} T N(\mu)$$

40

$$N(E) = \sum_{\mathbf{p},s} \delta(E - \varepsilon(\mathbf{p})) = 2 \int \frac{d^3p}{(2\pi\hbar)^3} \delta(E - \varepsilon(\mathbf{p}))$$

Consider a surface $S(\varepsilon)$ with $\varepsilon(\mathbf{p}) = const.$ and $d^3p = dS dp_n$ then

$$N(E) = \frac{2}{(2\pi\hbar)^3} \int_{\varepsilon = E} \frac{dS}{|\mathbf{v}(\mathbf{p})|}$$

39

Specific heat in metals

41

Definitions: Conjugation, isomorphic, linear representation, reducible, irreducible

42

Irreducible representations in quantum mechanics

43

Coupling of orthogonal orbitals

44

Intraband coupling of orbitals, derivation and result

45

Explain the band structure of p-orbitals using symmetry

46

Semiconductor vs. metal

47

Carrier density in insulators/semiconductors and metals

48

A conjugate to B if $A = XBX^{-1}$. Two groups are isomorphic if they have the same multiplication table. A linear representation of a Group G is a set of $n \times n$ matrices $D(G)$ which have the same multiplication table as the group itself.

$$D(G) = \begin{pmatrix} D_1'(G) & 0 \\ 0 & D_2'(G) \end{pmatrix}$$

Decomposable to block form $\Rightarrow$ reducible, and irreducible otherwise.

$C \sim TN(\mu)$: Only electrons in a narrow region around the Fermi surface participate in the thermal excitation. Linear temperature dependence typical for metals. For isotropic metal

$$N(\mu) = \frac{p_F m^*}{\pi^2 \hbar^3} \quad \Rightarrow \quad C = \gamma T$$

where $\gamma = p_F m^*/3\hbar^3$. Note that $m^* \sim p_F^2/\Delta\varepsilon$ and small orbital overlap in transition metals leading to large specific heat values.

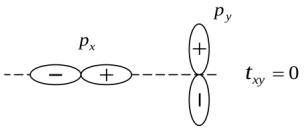

For nearest neighbour coupling orbitals with different symmetry do not mix and hence orthogonal orbitals do not couple. A mirror reflection is used to show this.

If G is the symmetry group of a Hamiltonian then $[H, G] = 0$. For ψ_n eigenstate of H, $G\psi_n$ is also an eigenstate with same energy. The eigenvectors form a representation of G provided that H is diagonal. The dimensionality gives the degree of degeneracy.

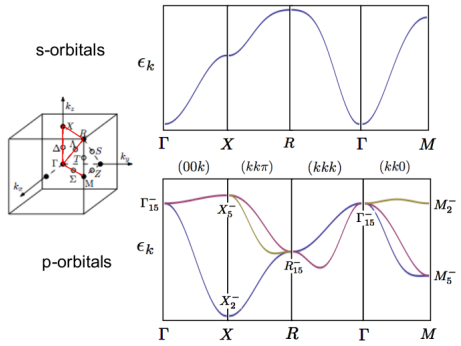

$$\mathcal{H} = E_p - \sum_{i,j} (t_{ij} c_i^\dagger c_j + h.c.)$$

Diagonalization by Fourier transformation, no mixing of bands for nearest neighbour. Including next nearest neighbour but only intraband coupling results in similar model but with anisotropy of hoppings. Including inter-band coupling mixes orbitals with different symmetry.

$$n = n_0 \left(\frac{T}{T_0}\right)^{3/2} e^{-E_g/2T}$$

For $E_g \sim 5.5eV \Rightarrow n \sim 10^{-27} cm^{-3}$ in insulators (diamond) and for $E_g \sim 0.5 - 1eV \Rightarrow$ $n \sim 10^5 - 10^{10} cm^{-3}$ which is $\ll n \sim 10^{23} cm^{-3}$ than for metals at room temperature.

Conductivity: $\sigma = ne^2\tau/m$ (Drude)

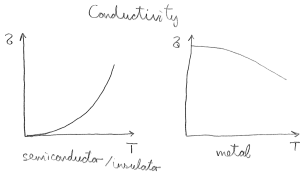

$n(T)$ | n is temperature independent, rather $\tau(T)$

Mobility (semiconductor)

49

Silicone general
Typical values in doped semiconductor

50

Gallium arsenide
Structure/Symmetry

51

Elementary excitations in semiconductors

52

Effective masses

53

Cyclotron resonance

54

Excitons

55

Optical properties of a semiconductor

56

Diamond structure: two intercalated fcc at (0, 0, 0) and (1/4, 1/4, 1/4). $2s$ and $2p$ hybridized. Has cubic symmetry. It has an indirect gap of 1.12 eV. Intrinsic at room temperature: $n_e = n_h \sim 10^{10} cm^{-3}$ and doped with a donor concentration $n_d \sim 10^{17} cm^{-3}$ one gets $n_e \sim 10^{17} cm^{-3}$ and $n_h \sim 10^3 cm^{-3}$ where

$$n^2(T) = n_0^2 \Big(\frac{T}{T_0}\Big)^3 e^{-E_g/T}$$

was used.

50

The conductivity of a semiconductor is not a good measure for the scattering rate. One rather uses the mobility μ with $v = \mu E$ and therefore the conductivity $\sigma = ne\mu$. The temperature dependence of conductivity mainly given by $n(T)$ is hence separated from the purity of the sampel characterized by μ.

49

Parabolic spectrum and $E_g - \mu \gg T$
Use Fermi function for n and conservation of electrons: $n_c + n_v = n$

$$\mu = \frac{E_g}{2} + \frac{3}{4} T \log\Big(\frac{m_v}{m_c}\Big)$$

For $T = 0$, μ is at the center of the band gap and the carrier density is

$$n_c \propto T^{3/2} e^{-E_g/2T}$$

52

Zinc blende structure: diamond with alternating types of atoms. Has cubic symmetry.

51

$\omega_c \tau \gg 1$ In presence of a static $\mathbf{B}$-field the e^- and hole motion is

$$m \frac{d\mathbf{v}}{dt} = \mp \frac{e}{c} \mathbf{v} \times \mathbf{B}$$

$\Rightarrow$ precession with cyclotron frequency $\omega_c = eB/mc$. Applying AC $\mathbf{E}$-field $\perp$ to $\mathbf{B}$ one gets resonance absorption at ω_c and measures the effective mass

$$m^* = \Big(\frac{\det(m_{\alpha\beta})}{m_{zz}}\Big)^{1/2}$$

54

$$\varepsilon_c(k) = E_g + \hbar^2 \Big(\frac{k_1^2}{2m_1^2} + \frac{k_2^2}{2m_2^2} + \frac{k_3^2}{2m_3^2}\Big)$$

is in general anisotropic, but for GaAs at $k = 0$ $m_1 = m_2 = m_3$ due to cubic symmetry in the top and the bottom of the band. In Si valence band meet at $k = 0$ with $M = 0.5 m_e$ and $m = 0.16 m_e$. They remain symmetric due to cubic symmetry. Beware: bottom of conduction band has lower symmetry $\Rightarrow$ different longitudinal and transverse masses.

53

Conductivity of a semiconductor can be enhanced by exciting electron-hole pairs via absorption of photons. But $\hbar\omega \sim E_g \Rightarrow k \ll 2\pi/a$ and therefore only leading to direct excitations. For semiconductors with an indirect energy gap phonon absorption/emission is required but the transition rate is reduced.

56

e^- and holes have opposite charge $\Rightarrow$ attraction and form a bound state with energy

$$E(k) = E_g - \frac{\mu_{ex} e^4}{2\varepsilon^2 \hbar^2 n^2} + \frac{\hbar^2 k^2}{2M_{ex}},$$

where μ_{ex} reduced mass, M_{ex} total mass. Typically exciton energy is $\sim 10^{-3}$ Ry.

55

Doping semiconductors

57

pn-junction

58

pn-junction functionality

59

pn-junction current

60

Light emitting diodes

61

Transistor

62

MOSFET

63

Orbital hybridization

64

A p-doped is brought into contact with an n-doped version of the same semiconductor. In equilibrium the chemical potential is constant. The depletion layer is

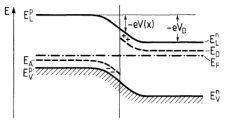

$d \sim 10^2 - 10^4 \text{Å}$

58

Donors (n-type): group V giving additional carriers. Acceptors (p-type): group III produce holes. An additional e^- results in a hydrogen atom like S.E. with an effective radius of 30 Å and hence forming an impurity band. The semiconductor can conduct in the impurity band by electron hopping from donor to donor. The chemical potential lies between the dopant level and the conduction band for n-doping.

57

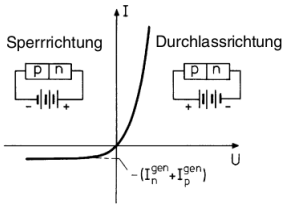

60

The e^- diffuse from the n-side to the p-side producing the diffusion current (same for holes). The electric field in the depletion layer produces the drift current in the opposite direction. In equilibrium these two currents compensate each other. Applying voltage that reduces the dipole field enhances the diffusion without changing the drift current. The opposite voltage will only change the width of the depletion layer without producing current.

59

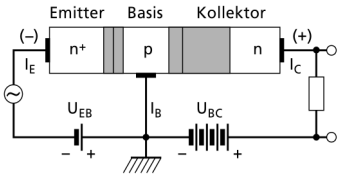

Active: EB open and BC closed ⇒ maximum amplification of the base current.

62

The recombination of electrons and holes can lead to the emission of photons with the frequency E_g. An excess of electron-hole pairs can be produced in pn-diodes by applying current. Different gaps allow to tune the color of the emitted light.

61

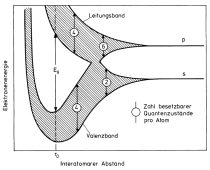

In diamond: $2s$ and $2p^3$ hybridize to sp^3 orbitals which is gapped from the conduction band. In graphene and graphite: three valence e^- occupy hybrid sp^2 orbitals to form three strong σ-bonds in a hexagonal structure. The remaining atom is perpendicular to the plane forming a π-bond.

64

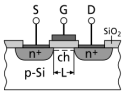

Apply gate voltage on the metal gate which is separated by insulating SiO_2. Applying gate voltage bends down the conduction band.

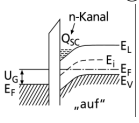

For sufficiently large voltage $eV_g > E_g$ an inversion layer is created providing carriers that connect source and drain producing large current.

63

π and σ bonding

65

Graphene derivation of energy dispersion

66

Dirac points

67

Density of states at a Dirac point in graphene

68

Cyclotron mass

69

Klein tunneling

70

Landau levels in graphene

71

Acoustic phonon branch, derivation

72

Tight binding model and nearest neighbours hopping

$$\mathcal{H} = -t \sum_{\mathbf{k},s} [\gamma(\mathbf{k}) a^\dagger_{\mathbf{k},s} b_{\mathbf{k},s} + \gamma^*(\mathbf{k}) b^\dagger_{\mathbf{k},s} a_{\mathbf{k},s}]$$

where $\gamma(\mathbf{k})$ is complex (lacks inversion symmetry). In matrix form and diagonalizing $\Rightarrow$ Dirac points

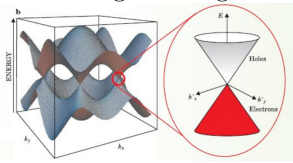

66

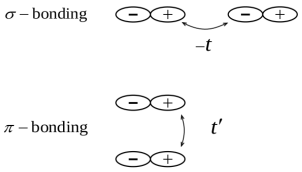

The π-bonding is usually weaker than the σ-bonding and is of the opposite sign.

65

$$N(E) = \frac{2}{(2\pi\hbar)^2} \int_{\varepsilon=E} \frac{dS}{|\partial\varepsilon/\partial p|}$$

and $\varepsilon = v_F|p|$ leads to

$$N(E) = \frac{E}{\pi(\hbar v_F)^2}$$

68

From $\varepsilon(\mathbf{k}) = \pm t|\gamma(\mathbf{k})|$ we get three K and three K' points with $\varepsilon(\mathbf{k}) = 0$. K and K' are not connected by a reciprocal lattice vector. Undoped graphene is a perfect semimetal, due to half filling. The spectrum near a Dirac point is

$$\varepsilon(\mathbf{p}) = \pm v_F|\mathbf{p}|$$

which results from solving the Dirac Hamiltonian $H = \hbar v_F \hat{\sigma} \cdot \mathbf{p}$.

67

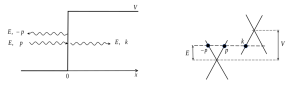

Solving the Dirac equation and using continuity at the boundary shows that the transmission coefficient is 1 and there is no reflection for a Dirac electron.

70

One can "dope" graphene by applying a gate voltage $\Rightarrow n_s = p_F^2/\pi\hbar^2$. The effective mass is given by

$$m^* = \frac{p_F}{|\partial\varepsilon/\partial p|} = \frac{\sqrt{\pi}\hbar}{v_F}\sqrt{n_s}$$

which can be measured in a cyclotron resonance experiment. Beware that the mass in a relativistic spectrum is not as simple as in parabolic dispersion.

69

Starting from a simple harmonic chain, small displacement expansion, go to Fourier space, periodic

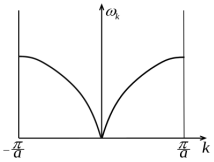

boundary conditions $\Rightarrow$
For $k \to 0$ (acoustic mode) we get linear spectrum and the particles are moving together.

72

Replace $\mathbf{p}$ by $\tilde{\mathbf{p}} = \mathbf{p} - e\mathbf{A}/c \Rightarrow$ Dirac Hamiltonian

$$\tilde{H} = \hbar v_F \hat{\sigma} \cdot \tilde{\mathbf{p}}$$

which is solved by considering $\mathcal{H}^2$ and results in

$$E = \pm\sqrt{2}\hbar v_F \left(\frac{eB}{c}\right)^{1/2} n^{1/2}$$

Compare this to the the usual Landau level quantization

$$E = \frac{\hbar eB}{mc}\left(n + \frac{1}{2}\right)$$

71

Optical phonon branch, derivation

73

Phonons transition of spectrum for equal masses in optical branch

74

Harmonic oscillator recap

75

Longitudinal and transverse sound

76

Planck's law

77

specific heat, phonon contribution

78

Dulong Petit law

79

Low temperature specific heat
Phonon contribution

80

Chain with alternating masses M_1 and M_2, go to Fourier space, solve for the frequency which has two solutions: an acoustic branch and an optical mode which does not go to zero for $k \to 0$. The particles are moving in the opposite directions. 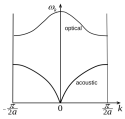

73

For $M_1 \neq M_2$ there is a gap and the zone boundary is at $\pi/2a$. The gap vanishes for $M_1 = M_2$ but the actual Brillouin stretches from $-\pi/a$ to π/a

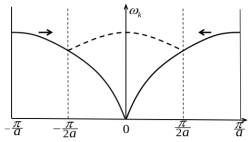

74

$$\mathcal{H} = \frac{\hat{p}^2}{2m} + \frac{\chi \hat{x}^2}{2}$$

with $\hat{p} = -i\hbar\partial/\partial x$, $[\hat{p}, \hat{x}] = -i\hbar$.

$$a, a^\dagger = \left(\frac{m\omega_0}{2\hbar}\right)^{1/2}\left[\hat{x} \pm \frac{i\hat{p}}{m\omega_0}\right]$$

which satisfy Bose commutation relations and the Hamiltonian $\mathcal{H} = \hbar\omega_0(a^\dagger a + 1/2)$ with ground state wave function $\psi(x) \propto exp(-m\omega_0 x^2/2l\hbar)$ and thus $\mathcal{H}\,|n\rangle = \hbar\omega_0(n + 1/2)\,|n\rangle$

75

$$\rho\ddot{\mathbf{u}} = \mu\boldsymbol{\nabla}^2\mathbf{u} + (\lambda + \mu)\text{grad div}\mathbf{u}$$

There are two kinds of waves, $\mathbf{u} = \mathbf{u}_l + \mathbf{u}_t$ where $\mathbf{u}_l$ satisfies $\text{rot}\mathbf{u}_l = 0$ with sound velocity $c_l = \sqrt{(2\mu + \lambda)/\rho}$ and $\mathbf{u}_t$ satisfies $\text{div}\mathbf{u}_t$ with sound velocity $c_t = \sqrt{\mu/\rho}$. There are one longitudinal and two transverse modes with dispersion $\mathbf{A_k} \parallel \mathbf{k}$, $\omega_l = c_l k$ and $\mathbf{A_k} \perp \mathbf{k}$, $\omega_t = c_t k$.

76

Bose statistics of phonons

$$\langle n_\omega \rangle = \frac{1}{e^{\beta(\varepsilon_\omega - \mu)} - 1}$$

The density of phonons is not fixed but determined by $\partial F/\partial N = 0 = \mu$ and hence we get Planck's law

$$\langle n_\omega \rangle = \frac{1}{e^{\beta\hbar\omega} - 1}$$

Alternatively use $E(n) = (n + 1/2)$.

77

The internal energy density is given by

$$E = \sum_k \hbar\omega_k(\langle n_k \rangle + 1/2) = \sum_k \frac{\hbar\omega_k}{2} + \frac{\hbar\omega_k}{e^{\beta\hbar\omega_k} - 1}.$$

Taking the derivative over temperature we obtain

$$C_v = \frac{\partial E}{\partial T} = \sum_k \frac{\partial}{\partial T}\frac{\hbar\omega_k}{e^{\beta\hbar\omega_k} - 1}.$$

78

Temperature higher than the maximal phonon frequency

$$\frac{1}{e^{\beta\hbar\omega_k} - 1} = \frac{1}{\beta\hbar\omega_k + 1/2(\beta\hbar\omega_k)^2 + ...} \approx \frac{T}{\hbar\omega_k}$$

$$C_v = \sum_k \frac{\partial}{\partial T}\hbar\omega_k \frac{T}{\hbar\omega_k} + ... = \sum_k 1$$

The total number of modes is 3 times the number of atoms N (phonons) and hence $C_v = 3N$.

79

$$C_v = V\frac{\partial}{\partial T}\sum_s \int_{\text{BZ}} \frac{d^3k}{(2\pi)^3}\frac{\hbar\omega_s(k)}{e^{\beta\hbar\omega_s(k)} - 1}$$

$$C_v = V\frac{\partial}{\partial T}\frac{T^4}{\hbar^3}\sum_s \int \frac{d\Omega}{(2\pi c_s(\hat{\mathbf{k}}))^3}\int \frac{x^3}{e^x - 1}dx$$

where $x = \hbar c_s(\hat{\mathbf{k}})k/T$ and integration of $k \in \mathcal{R}$

$$\frac{C_v}{V} = \frac{2\pi^2}{5}\left(\frac{T}{\hbar\bar{c}}\right)^3$$

80

Black body radiation

81

Debye model

82

Einstein model

83

Phonon density of states

84

Quick derivation of low temperature specific heat contributions

85

Anharmonicity and thermal expansion

86

Electron-phonon coupling

87

Phonon mediated attraction part I

88

Replace the full anisotropic spectrum by three single modes with $\omega = ck$ and replace the integration of the BZ with a sphere of radius k_D which has the same volume as the BZ. k_D defines $\omega_D = ck_D$ and $\Theta_D = \hbar\omega_D \sim 10^2 - 10^3$ K.

$$C_V = 9N\Big(\frac{T}{\Theta_D}\Big)^3 \int_0^{\Theta_D/T} \frac{x^4 e^x dx}{(e^x-1)^2}$$

82

The calculation of the specific heat contribution of phonons in the low temperature regime is almost identical to the derivation of the Stefan-Boltzmann law which is given by

$$E = \frac{\pi^2}{15}\frac{T^4}{(\hbar c)^3}$$

which differs by an additional factor of $2/3$ and $c_t = c$.

81

Replace integral over momenta by integral over phononic frequencies

$$\int \frac{d^3k}{(2\pi)^3} = \int d\omega g(\omega)$$

$$g(\omega) = \sum_s \int_{\omega_s(\mathbf{k})=\omega} \frac{dS}{(2\pi)^3}\frac{1}{|\partial\omega_s(\mathbf{k})/\partial\mathbf{k}|}$$

small frequencies: $\omega_s(k) \propto k$ and $g(\omega) \propto \omega^2$. As $\omega_s(k)$ has extrema in the BZ, it produces Van Hove singularities $g(\omega) \propto \sqrt{|\omega - \omega_0|}$.

84

Optical branch is replaced by the single frequency ω_E and spherical Brillouin zone. Each mode contributes

$$\frac{\hbar\omega_E}{e^{\hbar\omega_E/T}-1}$$

and the specific heat is

$$C_V^{opt} = 3N\Big(\frac{\hbar\omega_E}{T}\Big)^2 \frac{e^{\hbar\omega_E/T}}{(e^{\hbar\omega_E/T}-1)^2}$$

83

Interaction between atoms has cubic term and the frequencies in the phonon gas depend on volume.

$$F = \frac{1}{2}K\Big(\frac{\Delta V}{V}\Big)^2 + T\sum_{k,s}\log\Big[2\sinh\Big(\frac{\hbar\omega_s}{2T}\Big)\Big]$$

Taking derivative over ΔV

$$\alpha = \frac{\gamma}{K}c_v \propto T^3$$

at low temperatures.

86

Phonons are bosons and the energy is $\varepsilon \sim T$ and $\varepsilon \sim k$ $\Rightarrow \int d^3k \sim k^3 \sim T^3$. Multiplying by the energy and taking the derivative $\Rightarrow C_v \sim T^3$
Beware, lower dimensions yield different results.
Electrons are fermions and $\varepsilon \sim T$ and hence number of excitations $\sim N(\varepsilon_F)T$. Again multiplied by the energy T and taking the derivative gives $C_v \sim T$.

85

Electron-phonon interaction leads to an effective attraction between electrons. Lattice frequency is about Debye frequency $\omega_D \sim ck_F \sim \varepsilon_F\sqrt{m/M}$ and thus the ion trace is $L \sim a\sqrt{M/m}$. An electron moving in the opposite direction lowers the energy

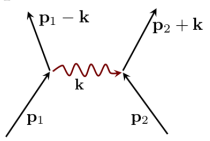

88

The strength of the electron phonon interaction is $V_{e-ph} \sim \varepsilon_F \mathrm{div}\mathbf{u}$, where the interaction with the longitudinal phonons are important.

$$\mathcal{H}_{e-ph} = \frac{i}{2}\sum \mathbf{q}(V_{-\mathbf{q}}\mathbf{u}_\mathbf{q} a^\dagger_{\mathbf{k}+\mathbf{q}} a_\mathbf{k} - V_\mathbf{q}\mathbf{u}_\mathbf{q} a^\dagger_\mathbf{k} a_{\mathbf{k}+\mathbf{q}})$$

The Hamiltonian corresponds to emission or absorption of phonons.

87

Phonon mediated attraction part II

89

Peierls transition

90

Derivation of gap in Peierls transition

91

Thomas Fermi approximation

92

Debye - Hückel screening

93

Plasma frequency

94

Lindhard function derivation

95

General expression for $\varepsilon(q, \omega)$

96

One-dimensional metal with half filling and lattice

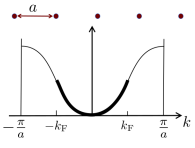

deformation by $u(x) = u_0 cos(Qx)$ The potential leads to a gap opening at $k = \pm Q/2$. If $Q = 2k_F$ there is a gain in energy as all the states below go further down in energy. Thus a 1-D metal is unstable with respect to a lattice deformation $\Rightarrow$ Charge density wave state.

90

The amplitudes of the two phonon-e^- scattering processes is

$$\sim \frac{\hbar^3}{p_F} \frac{\omega^2(\mathbf{k})}{(\omega^2 - \omega^2(\mathbf{k}))}$$

which is attractive for the energy transfer $\hbar\omega = \varepsilon(\mathbf{p}_1) - \varepsilon(\mathbf{p'}_1) < \omega(\mathbf{k})$. For $\omega \ll \omega(\mathbf{k})$ the interaction doesn't depend on $\mathbf{k}$ which corresponds to point like interaction. Important phonons are at $\omega(\mathbf{k}) \sim \omega_D$. The attraction occurs for e^- in a narrow layer near the Fermi surface with thickness $\hbar\omega_D$.

89

Spherical approximation, Jellium model, slowly varying electric field, constant chemical potential

$$\mu = \varepsilon_F(n_0 + \delta n(\mathbf{r})) - e\phi(\mathbf{r}) = \frac{\hbar^2}{2m}(3\pi^2 n_0)^{2/3}$$

Use Taylor, $\varepsilon_F \propto n_0^{2/3}$ and Poisson equation

$$\boldsymbol{\nabla}^2\phi - \frac{\phi}{\lambda_{\mathrm{TF}}^2} = -4\pi\rho_{\mathrm{ind}}$$

$\phi = Q\exp(-r/\lambda_{\mathrm{TF}})/r$. The coulomb interaction is screened on the Thomas Fermi length $\lambda_{\mathrm{TF}}^2 \sim 0.55$Å, $\lambda_{\mathrm{TF}} \sim k_F^{-1}$. $\varepsilon(\mathbf{q}, 0) = 1 + k_{TF}^2/q^2$.

92

Small deformation and different but similar tunneling amplitudes t_1 and t_2 Start from the tight binding approximation, go to Fourier space, $\mathcal{H}^2$ eigenvalues, include elastic energy and sum over all k states

$$\Delta(0) = 8te^{-1/g^2}$$

$\kappa \propto 1/g^2$ and thus for stiff lattice the gap is small.

91

Long wave dielectric response $\varepsilon(\omega, 0)$ of an electron gas can be obtained from $m\ddot{x} = -eE$ and $\varepsilon\mathbf{E} = \mathbf{E} + 4\pi\mathbf{P} \Rightarrow$

$$\varepsilon = 1 - \frac{\omega_p^2}{\omega^2}$$

$$\boldsymbol{\nabla}^2\mathbf{E} = \frac{1}{c^2}\frac{\partial^2\varepsilon\mathbf{E}}{\partial t^2} = -\frac{\omega^2}{c^2}\varepsilon(\omega)\mathbf{E}$$

$\omega < \omega_p \Rightarrow$ exponential decay. For $\omega > \omega_p \Rightarrow$ transparent and at $\omega = \omega_p \Rightarrow$ plasma resonance.

94

Classical electron gas

$$\delta n(\mathbf{r}) = n_0 e^{-U(\mathbf{r})/T} - n_0 \approx \frac{n_0 e\phi}{T}$$

leads to

$$\lambda_D^2 = \frac{T}{4\pi e^2 n_0}$$

93

$V = -e\phi \quad \Rightarrow \quad \phi_{\delta n}(\mathbf{q}, \omega) = -4\pi e/q^2 \delta n(\mathbf{q}, \omega)$. Random phase approximation ϕ_a

$$\phi = \phi_a(\mathbf{q}, \omega) - \frac{4\pi e}{q^2}\delta n(\mathbf{q}, \omega)$$

with $\delta n(\mathbf{q}, \omega) = -\chi_0(\mathbf{q}, \omega)e\phi(\mathbf{q}, \omega)$. Using $\phi(\mathbf{q}, \omega) = \phi_a(\mathbf{q}, \omega)/\varepsilon(\mathbf{q}, \omega)$

$$\varepsilon(\mathbf{q}, \omega) = 1 - \frac{4\pi e^2}{q^2}\chi_0(\mathbf{q}, \omega)$$

96

Adiabatic switching of weak time- and position dependent external potential.

$$\mathcal{H} = \sum_{\mathbf{k}} \varepsilon_{\mathbf{k}} c_{\mathbf{k}}^\dagger c_{\mathbf{k}} + \sum_{\mathbf{q}} V(\mathbf{q}, \omega) c_{\mathbf{k}+\mathbf{q}}^\dagger c_{\mathbf{k}}$$

Linear response EOM for the density operator $i\hbar d/dt\rho_{\mathbf{k},\mathbf{q}} = [\rho_{\mathbf{k},\mathbf{q}}, \mathcal{H}]$. Thermal average and $\langle\rho_{\mathbf{k},\mathbf{q}}\rangle \propto \exp(-i\omega + \eta t)$

$$\delta n_{\mathrm{ind}} = \frac{1}{\Omega}\sum_k \frac{n_{\mathbf{k}+\mathbf{q}} - n_{\mathbf{k}}}{\varepsilon_{\mathbf{k}+\mathbf{q}} - \varepsilon_{\mathbf{k}} - \hbar\omega - i\hbar\eta} V(\mathbf{q}, \omega)$$

95

Deriving Thomas Fermi screening from $\varepsilon(\mathbf{q}, \omega)$ as a limiting case

97

Friedel oscillations

98

Adiabatic continuity

99

Concept of quasiparticles, summary

100

Quasiparticle life time

101

Quasiparticle energy

102

Landau function

103

Fermi liquid: Compressibility and sound velocity

104

Induced charge of a point charge at the origin:

$$\delta n(r) \to \pi A n_{a0} \frac{\cos(2k_F r)}{r^3}$$

The total electron charge exactly compensates the induced charge.

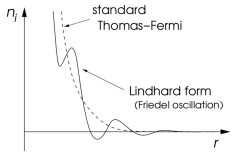

98

Static case $\omega = 0$

$$n_{\mathbf{k}+\mathbf{q}} = n_{\mathbf{k}} + \frac{\partial n}{\partial \varepsilon_{\mathbf{k}}} \mathbf{q} \cdot \boldsymbol{\nabla}_{\mathbf{k}} \varepsilon_{\mathbf{k}}$$

with $n_{\mathbf{k}}$ Fermi function at $T = 0$
$\partial n / \partial \varepsilon_{\mathbf{k}} = -\delta(\varepsilon_{\mathbf{k}} - \varepsilon_F)$

$$\chi_0(\mathbf{q}, \omega \to 0) = -\frac{1}{\pi} \frac{k_F^2}{\hbar v_F} = -\frac{3n_0}{2\varepsilon_F}$$

and thus $\varepsilon(\mathbf{q}, 0) = 1 + k_{\mathrm{TF}}^2/q^2$ with $k_{\mathrm{TF}}^2 = 6\pi e^2 n_0/\varepsilon_F$.

97

Weakly excited states of a system in a general case have energy level structure similar to the energy levels of an ideal gas. These elementary excitations (quasiparticles) are result of collective interaction of particle. The number of quasiparticles nor their statistics have to be the same as the number or statistics of the underlying particles. These excitations should have lifetime $\tau \ll \hbar/\varepsilon(p)$.

100

In the absence of phase transitions a non interacting ground state evolves smoothly or adiabatically into the interacting ground state as the strength of the interaction is increased. $\Rightarrow$ The low temperature properties of strongly interacting electrons are the same as those of non interacting fermions with renormalized parameters.

99

The quasiparticle energy $\varepsilon(k)$ is defined as the variational derivative of the total energy with respect to the quasiparticle distribution function

$$\delta E = 2V \int \varepsilon(k) \delta n(k) \frac{d^3k}{(2\pi)^3}$$

102

Fermi sphere and excitations similar to ideal gas: For $\varepsilon_1 = \varepsilon_F$ and ε_2 occupied (hence $\varepsilon_2 < \varepsilon_F$) as well as $\varepsilon_3, \varepsilon_4$ unoccupied ($\varepsilon_3, \varepsilon_4 > \varepsilon_F$) the allowed wave vectors are at the Fermi surface (by energy conservation) which has zero volume. For $\varepsilon_1 > \varepsilon_F$ and considering momentum conservation

$$\frac{\hbar}{\tau} \sim \frac{(\varepsilon_1 - \varepsilon_F)^2}{\varepsilon_F}$$

Energy quasiparticles $\sim T$. For $\varepsilon_F \sim$ eV, $T \sim 1$ K we get $l \sim$ cm mean free path. Scattering rate $\hbar/\tau \sim T^2 \varepsilon_F$

101

T= 0, use the expression for the effective mass and the definition $2F(\theta) = N(\varepsilon_F) f(\theta) \Rightarrow$

$$\frac{m^*}{m} = 1 + \langle F(\theta) \cos\theta \rangle_\theta$$

$$u^2 = \frac{k_F^2}{3mm^*}(1 + \langle F(\theta) \rangle)$$

104

$f(\mathbf{k}, \mathbf{k}') = f(\mathbf{k}', \mathbf{k})$ describes the interaction of two quasiparticles ($f = 0$ in Fermi gas). Using the Galilean invariance:

$$\frac{1}{m^*} = \frac{1}{m} - \frac{k_F}{(2\pi)^3} \int f(\theta) \cos\theta d\Omega$$

103

Pauli susceptibility in Fermi gas

105

Pauli susceptibility in Fermi liquid

106

Drude model

107

Drude model in AC-field

108

Reflectivity of a metal

109

Boltzmann equation

110

Drude from Boltzmann equation

111

Impurity scattering

112

Solution of the form $\delta\varepsilon = -\tilde{g}\mu_B\sigma\cdot\mathbf{H}$. In isotropic liquid: $f(\mathbf{k},\sigma;\mathbf{k}',\sigma') = f(\mathbf{k},\mathbf{k}') + \sigma\sigma'\zeta(\mathbf{k},\mathbf{k}')$. Recast this into

$$\delta\varepsilon = -\mu_B\sigma\cdot\mathbf{H} + \sum_{\sigma'}\int f(\mathbf{k},\mathbf{k}')\frac{\partial n_0'}{\partial\varepsilon'}\delta\varepsilon(\mathbf{k}',\sigma')\frac{d^3k'}{(2\pi)^3}$$

leads to

$$\chi = \mu_B^2\frac{N(\varepsilon_F)}{1+\langle Z(\theta)\rangle}$$

106

Fermi gas, g = 2, Zeeman term $\varepsilon(k) = \frac{k^2}{2m} - \mu_B g\mathbf{s}\cdot\mathbf{H}$ and the distributions (n_+) and (n_-) lead to

$$M = \frac{\mu_B}{2}\int_{\mu-\mu_B H}^{\mu+\mu_B H} N(\varepsilon)d\varepsilon$$

and using $M = \mu_B^2 N(\varepsilon_F)H$ finally

$$\chi_P = \mu_B^2 N(\varepsilon_F)$$

105

$\mathbf{E} = \mathbf{E}_\omega\exp(-i\omega t)$ leads to $1/\tau \to 1/\tau - i\omega$ and for absence of magnetic field $\sigma(\omega) = \sigma_0/(1-i\omega\tau)$. For an electric field varying in space and linear response equation one obtains using the Maxwell equations

$$\varepsilon(\omega) = 1 + \frac{4\pi i\sigma(\omega)}{\omega}$$

$\varepsilon(\omega)$ and $\sigma(\omega)$ satisfy the Kramers-Kronig relations.

108

$$m\frac{d\mathbf{v}}{dt} = -\frac{m\mathbf{v}}{\tau} + \mathbf{f}$$

Drude formula for conductivity: $\mathbf{j} = \sigma\mathbf{E}$ where $\sigma = ne^2\tau/m$. If magnetic field is present:

$$\mathbf{E} = \frac{m\mathbf{j}}{ne^2\tau} + \frac{\mathbf{j}\times\mathbf{B}}{nec}$$

with the Hall resistivity $\rho = B/nec$.

107

Semiclassical approximation, no spin Distribution function $df(\mathbf{k},\mathbf{r},t)/dt$ describes the change due to external fields.

$$\frac{\partial f}{\partial t} + \mathbf{v}\frac{\partial f}{\partial\mathbf{r}} + \mathbf{F}\frac{\partial f}{\partial\mathbf{k}} = I(f)$$

Ansatz with Isotropic, elastic scattering and $f = f_0 + f_1 \Rightarrow I(f) = -(f-f_0)/\tau$ (relaxation time approximation) $\Rightarrow$ integro-differential equation.

110

Use the wave equation and the boundary conditions at a transition into a metal. For $\omega\tau \ll 1 \ll \omega_p\tau \Rightarrow \varepsilon(\omega)$ is practically imaginary and the electric field decays inside the metal within the skin depth $\delta(\omega)$. For $1 \ll \omega\tau \ll \omega_p\tau \Rightarrow$ the field decays inside the sample within $\delta = c/\omega_p$ and $R \to 1$. For $\omega > \omega_p$ the reflectivity R drops to very small values. The shiny white arises from the fact that all of the visible frequencies are completely reflected since ω_p lies well above the visible light.

109

Fermi golden rule for scattering probability. τ is transport relaxation ($\neq \tilde{\tau}$ life time). Defects are point charges and Thomas-Fermi model for screened potential $\Rightarrow \sigma = ne^2\tau/m$. Beware: quadratic dependence of resistivity on the charge and temperature independence. This is called residual resistivity and vanishes for a perfect metal.

112

Relaxation time approximation, isotropic metal, elastic scattering, weak uniform electric field $(f = f_0 + f_1)$, $\partial f_0/\partial\varepsilon = -\delta(\varepsilon-\varepsilon_F)$
The Drude result is obtained:

$$\sigma = \frac{ne^2\tau}{m^*}$$

111

$e^- - e^-$ scattering contribution to conductivity

113

Electron-phonon interaction

114

Diffusion

115

Wiedemann-Franz law

116

Hall effect and magneto-resistance

117

High field Hall effect

118

Resistivity as a function of temperature

119

Relation: Brillouin zone and Fermi wave vector

120

Lifetime of quasiparticle in Fermi liquid:

$$\frac{1}{\tau} \simeq \frac{T^2}{\varepsilon_F}$$

hence $\sigma \simeq \frac{ne^2\varepsilon_F}{mT^2}$ and

$$\rho \simeq \frac{m\varepsilon_F}{ne^2}\left(\frac{T}{\varepsilon_F}\right)^2$$

which is temperature dependent.

113

High temperature: $\rho \sim mT/ne^2\hbar$
Low temperature: #phonons $\sim T^3$, scattering angle $\theta \sim T/\Theta_D$ and $\langle 1 - \cos\theta \sim T^2/\Theta_D^2 \Rightarrow$

$$\frac{1}{\tau_{e-p}} \sim T^5, \quad \rho \propto T^5$$

(Bloch-Grüneisen law)

114

Diffusion coefficient is defined by $\mathbf{j}_D = -D\boldsymbol{\nabla} n$ which in the case of electric current can be calculated to be

$$\mathbf{j} = eDN(\varepsilon_F)\mathbf{E}, \quad \sigma = e^2 DN(\varepsilon_F)$$

Einstein relation. $\partial f/\partial\varepsilon = -\delta(\varepsilon - \varepsilon_F)$ was assumed.

115

Relaxation time approximation:

$$\frac{\varkappa}{\sigma T} = \frac{\pi^2}{3e^2}$$

For inelastic scattering (phonons at low temperature), forward and back scattering have the same effect:

$$\frac{\varkappa}{\sigma T} \propto \left(\frac{T}{\Theta_D}\right)^2$$

116

E small ($f = f_0 + f_1$), relaxation time approximation, $\mathbf{B} \neq 0$

$$\mathbf{E} = \rho_0\mathbf{j} + \frac{e\tau}{mc}\rho_0[\mathbf{j} \times \mathbf{B}]$$

with Hall resistivity $\rho_{xy} = B/nec$, but absent magnetoresistance. If $\tau(\theta)$ depends on $\theta \Rightarrow$

$$\frac{\Delta\rho(B)}{\rho} \propto B^2$$

117

$T \ll \tau$, $\mathbf{B} \parallel \mathbf{z}$, $\mathbf{E} \parallel \mathbf{x}$ and $f_1 = ak_y$

$$e(\mathbf{E}\cdot\mathbf{v})\frac{\partial f_0}{\partial\varepsilon} = \frac{f_1}{\tau} - \frac{e[\mathbf{v}\times\mathbf{B}]}{c}\frac{\partial f_1}{\partial\mathbf{k}}$$

For closed and open electron-like Fermi-surface

$$\sigma_{xy} = -\frac{(n_e - n_h)ec}{B}$$

Closed:

118

Electron-electron in Fermi liquid: $\rho(T) \propto \rho_0 + AT^2$
Electron-phonon (Bloch Grüneisen):

$$\rho(T) = \begin{cases} \rho_0 + AT^5 & T < \Theta_D \\ T & T > \Theta_D \end{cases}$$

119

The Brillouin zone is defined as $-\pi/a < k < \pi/a$. In one dimension and one e^- per unit cell the Fermi wave vector is given by

$$k_F = \frac{\pi}{2a}$$

120

Anderson localization

121

One dimensional localization and Landauer formula

122

Thouless approach

123

Scaling theory of localization

124

Quantum corrections to conductivity

125

Quantum correction
Negative magneto-resistance

126

Variable range hopping

127

Landau levels

128

Transfer matrix equation $\Rightarrow \langle t \rangle = \prod t_n$ and transmission is a multiplicative function $\Rightarrow$ only transmission of unreflected waves contribute to total transmission $\Rightarrow$ resistance grows exponentially.

$$R = \frac{h}{e^2}\left|\frac{r}{t}\right|^2$$

and $R(L) = \pi\hbar/e^2 \exp(L/L_c)$.

122

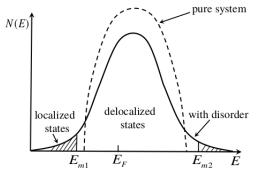

For strong disorder $E_{m1} \to E_{m2}$, all states are localized. If E_F crosses the mobility edge, we have the Metal Insulator transition.

121

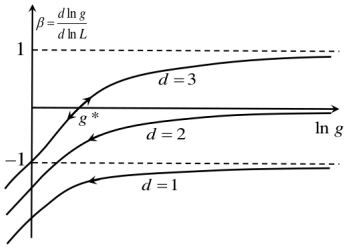

$L_c \sim l|x|^{-\nu}$ and $\sigma \sim \frac{e^2 g^*}{\hbar l} x^\nu$ close to the unstable fixed point g^*.

124

Consider two blocks where the coupling is $\sim E_c$ and the spacing between energy levels $\sim \Delta \Rightarrow$ tight binding model. If $E_c \gg \Delta$ then Ohms law. For $E_c \ll \Delta$ then localization. For a wire with small length $R < \hbar/e^2$ (quantum resistance 4 KΩ) and Ohms law. For length exceeding L_c we get $R \propto \exp(L/L_c)$, where $L_c \sim l(Sk_F^2)$.

123

For magnetic field: $\Psi \to \Psi \exp(\pm i\pi BS/\Phi_0)$ leading to

$$\delta G_d(H) - \delta G_d(0) \sim \frac{e^2}{\hbar}\begin{cases}\log(eBD\tau_\varphi/\hbar c) & d=2\\ (eB/\hbar c)^{1/2} & d=3\end{cases}$$

The appearance of a phase difference results in destruction of the interference, i.e., in a decrease of the resistivity.

126

$\lambda \ll l$ and $T \to 0$ Due to self intersection, interference is enhanced leading to a decrease in conductivity.

$$\delta G_d \sim -\frac{e^2}{\hbar}\begin{cases}L_\varphi & d=1\\ \log(L_\varphi/l) & d=2\\ 1/l - 1/L_\varphi & d=3\end{cases}$$

with $L_\varphi = \sqrt{D\tau_\varphi}$ and $\tau_\varphi \sim T^{-p}$. Note that that the divergence of L_φ supports localization in 1d and 2d. For $g \to \infty$ we obtain $\beta(g) = d - 2 - const/g$.

125

$\mathcal{H} = 1/2m(-i\hbar\boldsymbol{\nabla} - e/c\mathbf{A})^2$ leads to

$$\varepsilon = \frac{k_z^2}{2m} + \hbar\omega_c\left(n + \frac{1}{2}\right)$$

Discrete and highly degenerate Landau levels.

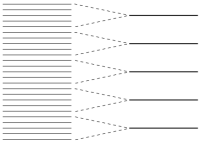

128

$E_F < E_{m1}$, conduction by hopping from localized states costs thermal energy and quantum tunnelling energy

$$P \propto \exp\left(-\frac{\Delta\varepsilon}{T} - \frac{2R}{L_c}\right)$$

optimizing R leads to $\sigma \propto \exp(T_0/T)^{1/(d+1)}$ (Mott's law) and including Coulomb energy $\sigma \propto \exp\left(-(T_1/T)^{1/2}\right)$ (Coulomb gap law).

127

Density of states in Landau level

129

Landau diamagnetism

130

Larmor (Langevin) susceptibility

131

Quantization of orbits

132

de Haas - van Alphen effect

133

Magnetism of localized spins

134

Band ferromagnetism

135

Landau theory of ferromagnetic transition

136

$$\chi_L = -\frac{\mu_B^2 N(\varepsilon_F)}{3}$$

Beware: Without Fermi liquid corrections, paramagnetic has free electron mass and Landau susceptibility has the band mass: $|\chi_L|/\chi_P = (m/m^*)^2/3$. Note that $\chi_P \sim 10^{-5}$.

130

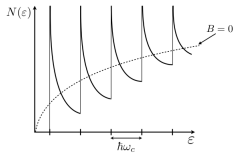

The degeneracy of a Landau level is equal to the total number of flux quanta threading the system.

$$N(\varepsilon, n) = \frac{(2m)^{3/2}\omega_c}{(2\pi\hbar)^2\sqrt{\varepsilon - \hbar\omega_c(n+1/2)}}$$

129

Use the Bohr-Sommerfeld quantization rule

$$\oint \mathbf{P}\cdot d\mathbf{r} = 2\pi\hbar(n+\gamma)$$

Comparing trajectories in real (S_n) and reciprocal (A_n) space leads to

$$A_n = (n+\gamma)\frac{2\pi\hbar eB}{c}$$

quantization of the orbit area in k-space.

132

Take magnetism of the closed and completely filled atomic shells into account.

$$\chi_a = -\frac{e^2}{6mc^2}\frac{N}{V}\langle r^2\rangle$$

Atomic contribution may well exceed Pauli and Landau contribution. Most diamagnetic nonsuperconducting material has $\chi_a \sim 10^{-4}$.

131

$M = \mu_B \tanh(\mu_B B/T)$ thus for $B \to 0$ we get $\chi = \mu_B^2/T$ (Curie law). In mean field approximation

$$\langle s\rangle = \frac{1}{2}\tanh\left(\frac{J\langle s\rangle + \mu_B B}{T}\right)$$

self-consistent mean field equation for $\langle s\rangle$. For $B = 0$, solve graphically and $T_c = J/2$. Close to T_c we get $\langle s\rangle \propto (T_c - T)^{1/2}$ and slightly above T_c

$$\langle s\rangle = \frac{\mu_B B}{2(T - T_c)} \qquad \text{(Curie Weiss law)}$$

134

Landau levels bring oscillatory behaviour in the DOS and hence oscillations in magnetization.

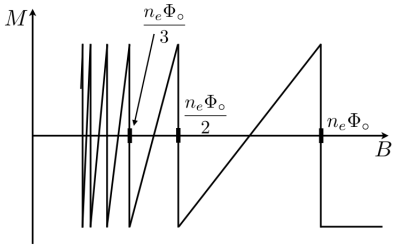

133

Close to the transition point

$$\mathbf{F}_L = a_0 + a_2(T)\mathbf{M}^2 + a_4\mathbf{M}^4$$

with $a_2(T) = a_2' t$, $t = (T - T_c)/T_c$ and finally for $B = 0$ we get $M \propto \sqrt{T_c - T}$ and

$$\chi_T(B) = \begin{cases} 1/2at & t > 0 \\ -1/4at & t < 0 \end{cases} \quad \text{Curie Weiss law}$$

and a jump in the specific heat.

136

Consider conduction electrons with a repulsive contact interaction (approximation of screened Coulomb interaction) and localized spin then

$$\mathcal{H} = \sum_{\mathbf{k},s}(\varepsilon_{\mathbf{k}} + un_{-s})c^\dagger_{\mathbf{k}s}c_{\mathbf{k}s} - UVn_\uparrow n_\downarrow$$

and assuming $m \ll n_0$ we get

$$\frac{UN(\varepsilon_F)}{2} = 1 \qquad \text{(Stoner criterion)}$$

For $UN(\varepsilon_F)/2 > 2$, transition to ferromagnetic state.

135

Mott transition estimate for critical density

137

Hubbard model

138

Mott - Hubbard transition
Figure/concept

139

Ground state of the Mott insulator

140

Classical antiferromagnet
Bipartite lattice

141

Landau theory of antiferromagnet

142

Replace Coulomb interaction with on site repulsion and half filling

$$\mathcal{H} = -t \sum_{i,j,s} (c_{is}^{\dagger} c_{js} + h.c.) + U \sum_{i} \hat{n}_{i\uparrow} \hat{n}_{i\downarrow}$$

Two limiting cases: $t = 0$ (insulating limit, highly degenerate 2^N states, first excited state is hole and one doubly occupied) and $U = 0$ (metallic state, $\varepsilon_k = -2t(\cos k_x a + \cos k_y a + \cos k_z a)$ with band width $W = 2zt = 12t$).

Compare kinetic energy $\varepsilon_{kin} = \hbar^2/m\lambda_{TF}$ to potential energy $\varepsilon_{pot} = e^2/\lambda_{TF}$ and use definition $\lambda_{TF} = \sqrt{r_0 a_0}/2$ and $a_0 = \hbar^2/me^2$ leading to

$r_0 > 4a_0$ insulating state

$r_0 < 4a_0$ metallic state

For a two-site Hubbard model at half filling there are two possible spin states in presence of a hopping t:

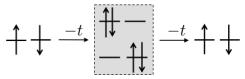

This superexchange process produces antiferromagnetic interaction

$$\mathcal{H} = J\hat{\mathbf{s}}_\mathbf{i} \cdot \hat{\mathbf{s}}_\mathbf{j}, \quad J = \frac{4t^2}{U}$$

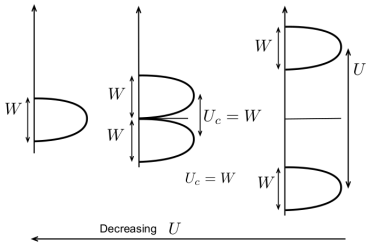

At half filling the lower Hubbard band is fully occupied ⇒ insulator.

Consider two sublattices, then magnetic response above T_N is isotropic in contrast to the magnetic response below T_N which depends on the orientation of the field $\mathbf{B}$.

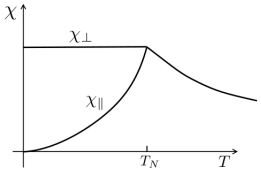

For bipartite lattice, the n.n. interaction can be presented as the interaction between the different sublattices. Introducing new spin variables leads to the ferromagnetic Heisenberg model. Thus transition temperatures as well as all thermodynamic properties in the absence of field are the same for ferro- and antiferromagnets on bipartite lattices. Note that the magnetic susceptibility does not diverge at T_N and $\langle s \rangle = \mu_B B/(T + T_N)$.